

Fe₃O₄/Polystyrene-Alginate Nanocomposite as a Novel Adsorbent for Highly Efficient Removal of Dyes

Mohammadi, Robab*⁺; Massoumi, Bakhshali; Mashayekhi, Ramin

Department of Chemistry, Payame Noor University, Tehran, I.R. IRAN

Hosseini, Akram

*Department of Engineering Science, College of Engineering, University of Tehran,
Tehran, I.R. IRAN*

ABSTRACT: *In this study, Fe₃O₄/polystyrene-alginate nanocomposite with high adsorption capacity was successfully prepared. Characterization of Fe₃O₄/polystyrene-alginate nanocomposite was carried out by various instruments, including SEM, EDX, FT-IR, XRD, and TGA. Then, the prepared nanocomposite was applied to remove malachite green as a cationic dye from aqueous solutions. The kinetic study was performed and the results showed the suitability of the pseudo-second-order kinetic model ($R^2 = 0.994$). The influence of different parameters, such as initial dye concentration, solution pH, adsorbent dosage, and contact time on the procedure was extensively investigated. The maximum adsorption of malachite green onto Fe₃O₄/polystyrene-alginate nanocomposite was found at an initial concentration of 20 mg/L, pH 7, adsorbent's dosage 500 mg/L, contact time equal to 20 min. To understand the nature of the adsorption procedure, the equilibrium adsorption isotherms were investigated. The linear correlation coefficients of Langmuir and Freundlich isotherms were obtained. The adsorption of malachite green was better fitted to Langmuir isotherm ($R^2 = 0.996$). According to the Langmuir isotherm model, the maximum adsorption capacity of Fe₃O₄/polystyrene-alginate nanocomposite for sequestering malachite green was about 90.81 mg/g. In addition, negative ΔG^0 and ΔH^0 values obtained through thermodynamic investigation implied that the adsorption of malachite green onto Fe₃O₄/polystyrene-alginate nanocomposite was simultaneous and exothermic in nature, respectively.*

KEYWORDS: *Fe₃O₄/polystyrene-alginate nanocomposite; Malachite green; Operational parameters; Adsorption isotherms; Thermodynamic investigation.*

INTRODUCTION

Environmental pollutants are regarded as one of the most important issues worldwide because of its harmful

and dangerous impact on ecosystems and human health[1]. The treatment of polluted wastewater can be carried out by

* To whom correspondence should be addressed.

+ E-mail: r.mohammadi@pnu.ac.ir

1021-9986/2022/11/3553-3566

14/\$/6.04

various physicochemical and biological procedures including adsorption, chemical oxidation, membrane technology, and Advanced Oxidation Processes (AOPs) [3–6]. Adsorption is one of the most effective treatment methods because of its simplicity and low cost. The main factor in an adsorption procedure is to select an adsorbent with strong capacity and fast kinetics for pollutant removal from wastewater [7]. Various adsorbents such as activated alumina, activated carbon, chitosan, and Alginate have been investigated in water treatment [8-10]. Alginate is one of the most extensively studied biopolymers generated from brown algae, which can be applied as a sorbent due to good hydrophilicity, low cost, nontoxicity, biocompatibility, and high adsorption potential to remove the pollutants. Furthermore, the adsorption capacity of the alginate for sequestering cationic dyes because of the electrostatic attraction between the carboxylate groups on the alginate and the ammonium groups of the cationic dyes would be beneficial to increase the adsorption of cationic dyes together with the immobilized adsorbent [11]. However, it is hard to separate the applied adsorbents from treated wastewater. So, Fe₃O₄-loaded adsorbents have attracted more attention because of their unique properties such as easy recovery through a magnet, large surface area, simple manipulation procedure, and high separation efficiency [12,13]. Fe₃O₄ nanoparticles may aggregate in the solution, which can decrease their surface area and affect stability and catalytic efficiency. Thus, surface modification for magnetic Fe₃O₄ nanoparticles is a necessity [14-16].

Polymers are frequently applied for surface modification of Fe₃O₄ nanoparticles because of several advantages that make them suitable in catalytic applications. For instance, polymer coatings can be generated to change the surface properties of superparamagnetic nanoparticles, to increase the compatibility between nanoparticles and aqueous medium, to avoid particle surface from oxidation, to decrease toxicity and to facilitate storage or transport, to physically adsorb materials [17].

The main subject of this study is the synthesis of Fe₃O₄/polystyrene-alginate nanocomposite and the evaluation of its adsorption capacity for the removal of a cationic dye (malachite green) in aqueous solutions. To the best of our knowledge, there is no report on the preparation and application of Fe₃O₄/polystyrene-alginate nanocomposite as an adsorbent for the elimination of textile dyes.

Different adsorption factors such as contact time, adsorbent dosage, dye concentration, and pH of the solution were studied. Moreover, kinetics (pseudo-first and pseudo-second order), equilibrium isotherms (Langmuir and Freundlich models), and thermodynamic investigations were used in this study. The search for new alternative, inexpensive, eco-friendly, and efficient adsorbents to replace the commercially available adsorbents is ongoing.

EXPERIMENTAL SECTION

Chemicals

Iron (III) chloride hexahydrate (FeCl₃·6H₂O), iron (II) sulfate heptahydrate (FeSO₄·7H₂O), xylene (≥ 99.0 %), ammonium hydroxide (28% v/v, NH₃·H₂O), and calcium chloride anhydrous powder (CaCl₂) are of analytical grade and are obtained from Merck, Germany. Polystyrene (PS, M_w 35×10³), and sodium alginate (CAS no. 9005-38-3) were obtained from Sigma Aldrich. Malachite green was purchased from Alvan sabet Co., Iran and used without further purification.

Preparation of Fe₃O₄ nanoparticles

Fe₃O₄ nanoparticles were prepared via the reverse co-precipitation method using ammonia as a precipitation agent. In short, 5 mL of 1 mol/L FeCl₃·6H₂O solution and 10 mL of 0.5 mol/L FeSO₄·7H₂O solutions were mixed. The mixture was added dropwise into 20 mL of 3.5 mol/L ammonium hydroxide solution at 60 °C under ultrasound irradiation. The reaction proceeded for 30 min and the overall reaction of Fe₃O₄ is expected as follows [21]:



Upon completion of the reaction, the resulting black iron oxide nanoparticles were collected with the help of a strong magnet and washed several times with distilled water (Millipore–Aquelix, USA).

Preparation of Fe₃O₄/polystyrene nanocomposite

For Fe₃O₄ /polystyrene nanocomposite preparation, 0.1 g polystyrene (Sabic company) was dissolved in 5 mL xylene. Also, 0.5 g Fe₃O₄ was dispersed in 5 mL xylene for 20 minutes in an ultrasonic bath and added dropwise into the above solution under continuous stirring. The final product was mechanically stirred for 2 hours. Finally, the resulting nanocomposite was washed twice with 30 mL water and dried at 50 °C.

Preparation of Fe₃O₄/polystyrene-alginate nanocomposite

Fe₃O₄/polystyrene-alginate nanocomposite was prepared in cross-linking solution using calcium chloride as cross-linking agent. In a typical procedure, prepared Fe₃O₄/polystyrene nanocomposite was dispersed in 100 mL of water and then, 0.2 g of sodium alginate were added to it. The suspension was mixed for 4 h, then added drop wise into a mixture of calcium chloride and ferrous sulfate under continuous stirring. Fe₃O₄/polystyrene-alginate was formed instantly. The formed nanocomposite was left in the solution for 2 h. It was then collected with a magnet and washed several times with distilled water to remove the excess of unreacted materials. Finally, Fe₃O₄/polystyrene-alginate nanocomposite was dried at 60 °C.

Characterization

The morphology and texture of Fe₃O₄/polystyrene-alginate nanocomposite were measured *via* a Scanning Electron Microscope (SEM) (Philips XL-30ESM). The chemical composition of the synthesized nanocomposite was analyzed by an Energy Dispersive X-ray (EDX) spectroscopy system. Fourier Transform InfraRed (FT-IR) spectroscopy analysis of nanocomposite was performed on a Nicolet 560 FT-IR spectrometer. The sample was prepared by mixing it with KBr and pressing it into a compact pellet. The crystal structure and the crystallite size of the prepared sample was recorded using X-Ray Diffraction (XRD) (Siemens/D5000) with Cu K α radiation (0.15478 nm) in the 2 θ scan range of 10°–70°. The average crystallite size (D in nm) was calculated using Scherrer's formula [22]:

$$D = \frac{k\lambda}{\beta \cos\theta} \quad (2)$$

where k is a constant equal to 0.89, λ , the X-ray wavelength equal to 0.154056 nm, β , the full width at half maximum intensity (FWHM) and θ , the half diffraction angle. ThermoGravimetric Analyses (TGA) were carried out by a TGA apparatus (NETZSCH-GERÄTEBAU GMBHSTA 409 PC LUXX, Kerman, Iran). TGA was measured in the temperature range of 800° C at a heating rate of 10 °C/min under N₂ atmosphere.

Batch experimental system

The experiments were performed in 100 mL Erlenmeyer flasks as batch experimental reactors to evaluate the effects of operational parameters such as the

reaction time, adsorbent dosage, initial pH and the initial dye concentration on malachite green adsorption onto Fe₃O₄/polystyrene-alginate nanocomposite. In each run, desired concentration of malachite green and Fe₃O₄/polystyrene-alginate nanocomposite were fed into the quartz and allowed to establish an adsorption–desorption equilibrium for 30 min and then mixed by shaking at a temperature of 25 °C. The pH was adjusted to the desirable values with 0.1 M HCl and 0.1 M NaOH at the beginning of each experiment. The set of experiment was conducted at an initial dye concentration of 20 mg/L, adsorbent dosage of 500 mg/L and initial pH of 7 for 20 min. Then, the experimental procedure was systematically performed according to Table 1. Subsequently, a magnet was used to collect the magnetic nanocomposite and the adsorption was monitored by UV-Vis Perkin-Elmer 550 SE spectrophotometer at wavelength of 617 nm. All experiments were carried out twice to check the accuracy of the obtained data. Then the mean values were written down. The amount of malachite green adsorbed onto Fe₃O₄/polystyrene-alginate was calculated via Eq. (3):

$$q = \frac{(C_0 - C) V}{M} \quad (3)$$

Where q , C_0 and C are the amount of adsorbed malachite green (mg/g), the initial concentration and the final concentration of dye in the solution (mg/L), respectively. In addition, V is the volume of the solution (L) and M is the weight of the nanocomposite (g) [23].

RESULTS AND DISCUSSIONS

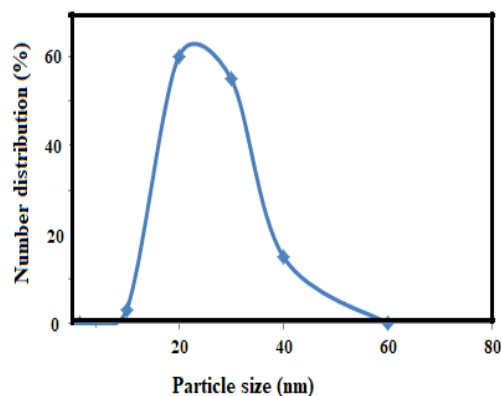
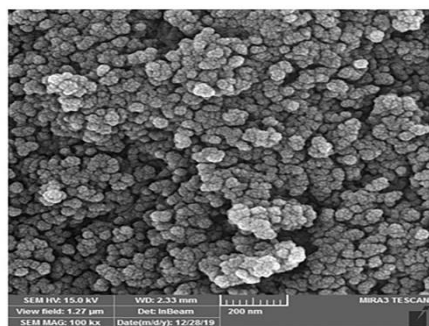
Characterization of prepared nanocomposite

Morphology and Particle Size

To investigate the morphology of the prepared nanocomposite, SEM technique was used. The SEM image of Fe₃O₄/polystyrene-alginate nanocomposite is shown in Fig.1 (a). The cubic and averagely spherical magnetite nanoparticles with very neat arrangement can be seen in this image. The SEM image shows that the prepared nanocomposite has a homogeneous morphology. This homogeneity can be achieved via alginate acting as a stabilizer for Fe₃O₄/polystyrene in the solution state, which in turn prevents the nanoparticles from aggregation [24]. The average size of the nanospheres was calculated based on the statistical size of at least one hundred particles. The particle size distribution of Fe₃O₄/polystyrene-alginate

Table 1: Experimental design for the adsorption of malachite green onto Fe_3O_4 /polystyrene-alginate nanocomposite.

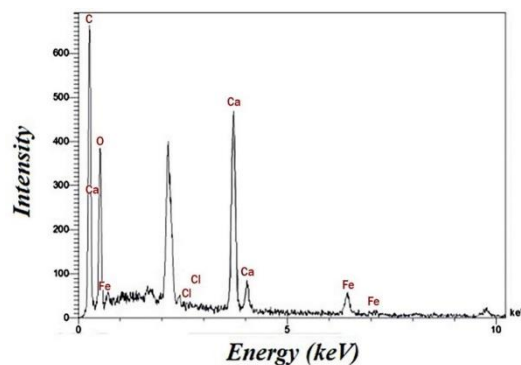
No. Parameter	Reaction time (min)	Adsorbent dosage (mg/L)	Initial pH	Dye concentration (mg/L)
Reaction time	0-30	500	Neutral	20
Adsorbent dosage	20	100-600	Neutral	20
pH	20	500	3-8	20
Dye concentration	20	500	Neutral	20-100

**Fig. 1: (a) SEM image of Fe_3O_4 /polystyrene-alginate. (b) Size distribution of Fe_3O_4 /polystyrene-alginate.**

nanocomposite is shown in Fig. 1 (b). It is revealed that Fe_3O_4 /polystyrene-alginate nanocomposite yields mainly nanoparticles with a diameter of 15-50 nm, with the highest contribution of 20–30 nm, in an amount of 63%. The sample shows a single broad peak, which seems that Fe_3O_4 -alginate is completely encapsulated in polystyrene particles. From the above mentioned, therefore, Fe_3O_4 /polystyrene-alginate nanocomposite has good morphology and particle size [25].

Elemental analysis with EDX spectroscopy

Energy dispersive X-ray spectroscopy analysis was used to identify elements, which exist in the prepared Fe_3O_4 /polystyrene-alginate nanocomposite. Fe, C, O, Ca, and Cl peaks can be clearly seen from Fig. 2. This result is considered as evidence for the even dispersion of Fe_3O_4 nanoparticles in the polystyrene matrix. Such fine dispersion of the nanoparticles could be causing the enhancement of the thermal stability of the investigated Fe_3O_4 /polystyrene-alginate nanocomposite and it will be discussed afterward. Energy dispersive X-ray spectroscopy analysis showed no significant levels of impurities, which could have originated from the procedure [26].

**Fig. 2: EDX pattern of Fe_3O_4 /polystyrene-alginate nanocomposite.**

FT-IR spectra of prepared samples

Typical FT-IR spectra of Alginate, Fe_3O_4 , Polystyrene, and Fe_3O_4 /polystyrene-alginate samples are shown in Fig. 3. Alginate (Fig. 3(a)) showed an intense band around $3300-3362\text{ cm}^{-1}$, which is attributed to the stretching of O-H. The spectral band around $2923-2854\text{ cm}^{-1}$ is attributed to stretch vibration absorption of aromatic and aliphatic C-H, respectively. The bands at 1625 cm^{-1} and 1425 cm^{-1} are associated with the asymmetric and symmetric vibration of COO^- groups, respectively. The peak appearing at 1042 cm^{-1} is assigned to the C-O-C stretching

vibration. The C-O stretching vibration of uronic acid residues is generally linked to the bands centered at 930 cm^{-1} . The signals at 815 cm^{-1} were attributed to mannuronic acid residues [27, 28]. The FT-IR spectrum of Fe_3O_4 nanoparticles is shown in Fig. 3(b). The peak at 3410 cm^{-1} is due to O-H stretching vibration arising from hydroxyl groups from the water on nanoparticles. The absorption peaks at 2926, 2860, 1628, and 1385.22 cm^{-1} are due to water used as solvent. The 785 and 578 cm^{-1} absorption peaks correspond to the Fe-O bond vibration of Fe_3O_4 nanoparticles [29]. The FT-IR spectrum of Polystyrene is shown in Fig. 3(c). The three adsorption peaks at 1425, 1492, and 1591 cm^{-1} are due to the vibration of C=C bonds in the benzene ring. Also, the double peaks at 756 and 696 cm^{-1} show that the benzene ring is singly substituted. The bands at 3026 cm^{-1} , 2850, and 2920 cm^{-1} are assigned to the stretch vibration absorption of aromatic and aliphatic C-H, respectively [30]. Fig. 3(d) shows the FT-IR spectrum of Fe_3O_4 /polystyrene-alginate nanocomposite. The strong absorption band that appeared at about 574 cm^{-1} is assigned to the vibrations of the Fe-O bond, which confirm the formation of Fe_3O_4 nanoparticles. The C-O stretching vibration of uronic acid residues is generally linked to the bands centered at 930 cm^{-1} . The signals at 815 cm^{-1} were attributed to mannuronic acid residues. The three adsorption peaks at 1591, 1425 and 1492 cm^{-1} are due to the vibration of C=C bonds in the benzene ring. Also, the double peaks at 756 and 698 cm^{-1} show that the benzene ring is single-substituted. The bands at 1602 cm^{-1} and 1438 cm^{-1} are associated with the asymmetric and symmetric vibration of COO^- groups, respectively. The band at 3020 cm^{-1} and $2848\text{-}2973\text{ cm}^{-1}$ are assigned to the stretch vibration absorption of aromatic and aliphatic C-H, respectively. The peaks at 3433 cm^{-1} , 1666, and 1031 cm^{-1} are related to the O-H stretching vibration, the C=O stretching vibration, and C-O stretching vibrations, respectively. Moreover, the broadening of the peak associated with O-H at 3433 cm^{-1} indicates the increased hydrogen bonding interactions due to the presence of Fe_3O_4 nanoparticles [31, 32]. Based on the above observation, we can find that the Fe_3O_4 nanoparticles, alginate, and polystyrene exist in the composite particles.

X-ray diffraction

The X-ray diffraction patterns of the prepared nanocomposite is shown in Fig. 4. The stacked

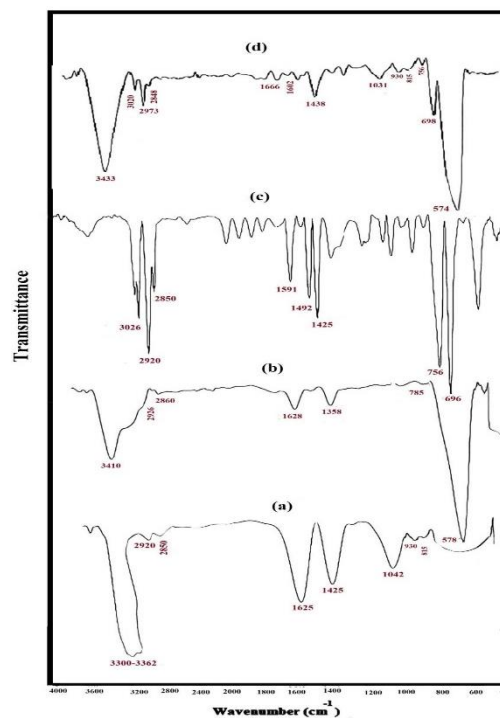


Fig. 3: FT-IR spectrum of Fe_3O_4 /polystyrene-alginate nanocomposite.

diffraction pattern shows no remarkable peaks for the alginate fibers. Each diffraction peak of the sample could be assigned to the cubic phase structure (JCPDS 019-0629). The peaks at 2θ values: 30.5, 35.6, 43.5, 53.8, 57.2 and 63.4° , could be indexed as the (220), (311), (400), (422), (511), and (400) crystal planes of cubic phase Fe_3O_4 , respectively [33].

The sharpness of the peaks clearly shows that the synthesized particles had a highly crystalline nature. These crystalline entities show the typical pattern of Fe_3O_4 , and there was no other phase such as Fe_2O_3 or $\text{Fe}(\text{OH})_3$, which were the usual co-products in the chemical reverse coprecipitation process. The peak positions of Fe_3O_4 nanoparticles are unchanged after encapsulation by polystyrene, which illustrated that the crystalline structure of Fe_3O_4 nanoparticles was not changed during the preparation procedure of Fe_3O_4 /polystyrene particles [34]. The broadening of the diffraction peaks indicates the nanoparticle nature of the sample. The average crystallite size was estimated from the line width of all diffraction peaks using the Debye-Scherrer formula which gives

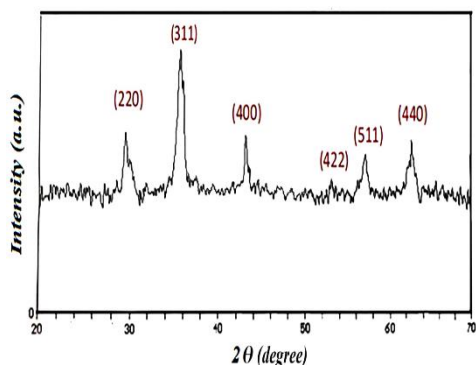


Fig. 4: XRD pattern of Fe₃O₄/polystyrene-alginate nanocomposite.

a relationship between peak broadening in XRD and particle size. The crystallite size thus obtained from this equation was found to be about 14.5 nm.

Thermal analysis

Fig. 5 shows the thermal behavior of Fe₃O₄/polystyrene-alginate nanocomposite. The thermogram clearly shows that the presence of Fe₃O₄ nanoparticles makes the system more thermally stable at a lower temperature. The different stages of thermal degradation of prepared nanocomposite could be observed as a multistep process. This figure shows three stages of weight loss. In I stage, from 0° C - 150° C, the slow weight loss (6.96 %) is attributed to evaporation of solvent trapped between the polymer chains. The second weight loss is about 28.1 % from 150° C - 450° C that can be assigned to the degradation of alginate. This fraction involves the side chains and the ester bonds connecting the monomeric units of the alginate [35]. The rapid weight decrease (83 %) is in the third region from 550° C - 750° C, which is attributed to the decomposition of the polystyrene polymer matrix. The residual weight should be related to the weight of Fe₃O₄. All adsorption experiments were carried out below 150° C. So, the slow weight loss shows the high thermal stability of nanocomposite. Moreover, the increased thermal stability of Fe₃O₄/polystyrene-alginate results from the interaction between polystyrene matrix and the Fe₃O₄ nanoparticles. The surface of the Fe₃O₄ nanoparticles absorbs the free radicals generated in the decomposition of polystyrene and limits the mobility of the molecules, which retards the degradation of the Fe₃O₄/polystyrene-alginate.

Adsorptive removal of malachite green by prepared samples

Fig. 6 displays the adsorptive removal of malachite

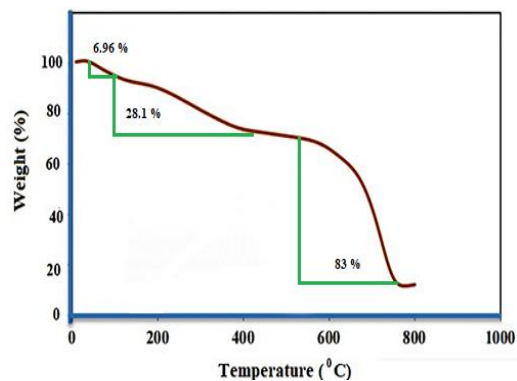


Fig. 5: TGA curve of Fe₃O₄/polystyrene-alginate nanocomposite.

green from aqueous solution using Fe₃O₄, Fe₃O₄/polystyrene and Fe₃O₄/polystyrene-alginate samples. It could be seen that Adsorptive removal of malachite green in the presence of Fe₃O₄/polystyrene is higher than pure Fe₃O₄. Studying the mechanism of adsorption via the nanomaterials depends on the outer coating of these nanostructures. Polystyrene was investigated as an outer coating in this nanomaterial. Its structure consists of a long chain hydrocarbon where the center carbons are bonded to benzene rings. It is well known that aromatics are very stable compounds. Therefore, the change in the structure of polystyrene is not easily accomplished. To study the adsorption procedure via nanomaterials, several parameters such as effective surface area should be considered. The mechanism of adsorption is dominated via physical procedure involves the electrostatic interaction between the ion in the solution and solid adsorbent, which is usually associated with low adsorption heat [36]. Ohsawa *et al.* studied Zeta potential and surface charge density of polystyrene-latex and found that there are 2000–4000 negative charges on its surface at pH=7.34 [37]. In other words, polystyrene-based adsorbents could show strong electrostatic interactions with positively charged species.

Also, Fig. 6 shows that Adsorptive removal of malachite green in the presence of Fe₃O₄/polystyrene-alginate is higher than Fe₃O₄/polystyrene. Accumulation of a substance between the liquid–solid interface or gas–solid interface because of physical or chemical associations is defined by the term the adsorption process. The adsorption process can be controlled via physical factors on most of the adsorbents such as polarity, Van der Waals forces, hydrogen bonding, dipole-dipole interaction,

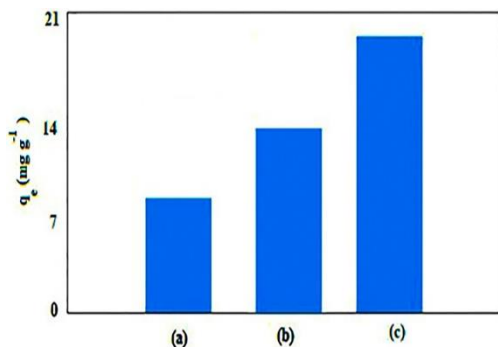


Fig. 6: Adsorptive removal of malachite green from aqueous solution in the presence of (a) Fe_3O_4 , (b) $Fe_3O_4/polystyrene$, and (c) $Fe_3O_4/polystyrene-alginate$ samples.

π - π interaction, etc. [38]. Therefore, the design of an adsorbent can be depended on the type of substance to be adsorbed or removed. Malachite green is a cationic dye that can be removed by an adsorbent showing a strong affinity toward positively-charged molecules. Due to the dissociation of carboxyl groups, the alginate-based catalyst was negatively charged and showed strong electrostatic interactions to positively charged species [39]. Based on results, the presence of alginate in prepared nanocomposite plays a crucial role in the removal of cationic dye from aqueous solutions [40].

Effect of contact time and kinetic study

The exposure time was varied between 0 and 30 min to investigate the influence of reaction time on the adsorption of malachite green. The results are shown in Fig. 7. Within the exposure time of 30 min, the adsorbed malachite green by $Fe_3O_4/polystyrene-alginate$ nanocomposite reached to 18.36 mg/g. The removal of malachite green *via* adsorption onto $Fe_3O_4/polystyrene-alginate$ nanocomposite was very fast during the initial contact time and then slowed down. This phenomena could be attributed to the sufficient exposure of adsorptive sites and the appropriate surface reactivity of the adsorbent for sequestering pollutant cations [41]. It can be seen from Fig. 7 that the enhancement in reaction time up to 20 min led to a little increase in adsorbed malachite green. With passage of time, the remaining vacant surface sites are difficult to be occupied because of the repulsive forces between the solute molecules on the solid phase and in the bulk liquid

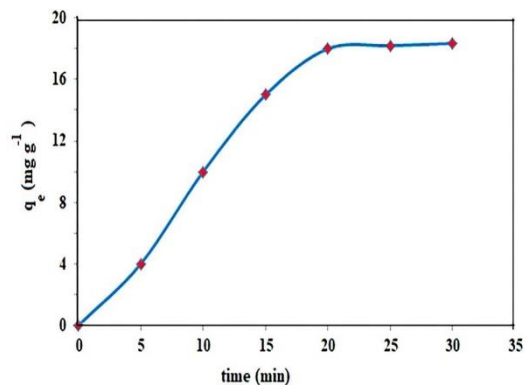


Fig. 7: Effect of contact time on malachite green adsorption onto $Fe_3O_4/polystyrene-alginate$ nanocomposite.

phase [42]. So, a reaction time of 20 min was selected as the optimal value for further experiments.

The kinetic investigation is very important in modeling and designing the full-scale adsorption plant [39]. The pseudo-first and pseudo-second-order kinetic models, as the most widely applied models, were used to assess the mechanism of the adsorption. The linear form of the pseudo-first-order kinetic model is as Eq. (4):

$$\log(q_e - q) = \log q_e - \left(\frac{k_{1,ads}}{2.303} \right) t \quad (4)$$

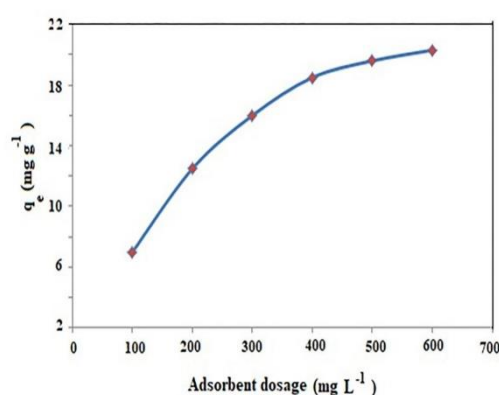
Where q (mg/g) and $k_{1,ads}$ (min⁻¹) are the amount of adsorbed dye at time t and the rate constant, respectively. The linear form of the pseudo-second-order kinetic model is presented as Eq. (5):

$$\frac{t}{q} = \frac{1}{k_{2,ads} q_e^2} + \left(\frac{1}{q_e} \right) t \quad (5)$$

where $k_{2,ads}$ (g/mg.min) is the rate constant of the equation [40]. The values of the pseudo-first and pseudo-second order kinetic parameters were calculated from the slope and intercept of linear plots of $\log(q_e - q)$ versus t and t/q versus t , respectively (The figures are not shown). From the slopes and intercepts, the values of $k_{1,ads}$ (min⁻¹), q_e and $k_{2,ads}$ were calculated and exhibited in Table 2. The kinetic of adsorption was investigated at an initial malachite green concentration of 20 mg/L, adsorbent dosage of 500 mg/L, initial pH of 7.0 and a contact time of 20 min. The correlation coefficient of the pseudo-second order model was more than that of pseudo-first order model for malachite green adsorption onto

Table 2: Kinetic parameters for malachite green adsorption onto Fe₃O₄/polystyrene-alginate nanocomposite.

Value	Type of kinetic model
Pseudo-first order model	
q _e (mg g ⁻¹)	28.84
k _{1,ads} (min ⁻¹)	0.102
R ²	0.984
Pseudo-second order model	
q _e (mg g ⁻¹)	34.12
k _{2,ads} (g mg ⁻¹ min ⁻¹)	0.154
R ²	0.994

**Fig. 8: The effect of adsorbent dosage on the adsorption of malachite green through Fe₃O₄/polystyrene-alginate nanocomposite.**

Fe₃O₄/polystyrene-alginate nanocomposite (R² = 0.994). The kinetics of the adsorption procedure may fit the pseudo-first-order model if dye adsorption is controlled *via* diffusion through a boundary layer. However, the adsorption procedure usually involves various mechanisms such as electrostatic and chemical interactions between binding sites and pollutant ions. So, the pseudo-second-order model provides the best fit for the adsorption procedure by various adsorbents [43].

Effect of adsorbent dosage

Fig. 8 displays the influence of adsorbent dosage on the amount of adsorbed malachite green. As shown in the graph, for the removal of malachite green, the adsorbent amount enhanced while the adsorption of pollutant enhanced, reaching a plateau value after a certain value. After this plateau value, the enhancement in the amount of

adsorbent does not significantly influence the adsorption. After this point, because of the fact that the adsorption event was an equilibrium event, there was no significant effect of enhancing the amount of adsorbent on the pollutant removal. The enhancement in percent removal of adsorbate ions with enhancement in the adsorbent dose could be related to more availability of adsorption sites [44]. At equilibrium, the percent removal became constant probably due to the saturation of the available adsorption sites. Equilibrium was attained at an adsorbent dosage of 500 mg/L. No considerable enhancement in the adsorption of malachite green with enhancing adsorbent dosage up to a given value can be related to the change in the concentration gradient of pollutant species between the bulk solution and adsorbent [45]. Thus, an adsorbent dosage of 500 mg/L can be chosen as selective value for subsequent experiments.

Effect of dye concentration

The effect of various initial dye concentration values, i.e., 20, 40, 60, 80, and 100 mg/L on the adsorption of malachite green in an aqueous solution was examined (Fig. 9). The results highlight that adsorbed malachite green slowed down with the higher-concentration solutions of dye. At a higher malachite green concentration, the surface of the catalyst was rapidly saturated and the malachite green adsorption intervened in the electron transfer procedure, subsequently decreasing the catalytic performance. Additionally, dye molecules and intermediates were competing for limited surface-bound radicals and reactive species on the catalyst surface under the higher concentrations of malachite green, thus preventing the overall decomposition efficiency of dye [46].

Effect of pH

Solution pH can play a significant role in the adsorption procedure influencing on other parameters such as adsorbent surface charge and ionization of functional groups presenting on the active site of the adsorbent surface [47]. The pH of aqueous solution is known as an important control factor in the adsorption procedure, because the bonding of cations to the surface groups can be depended on the surface charge of the particles. According to Fig. 10, adsorbed malachite green was increased with increasing initial pH. At higher pH, the adsorbent surface can be more negatively charged

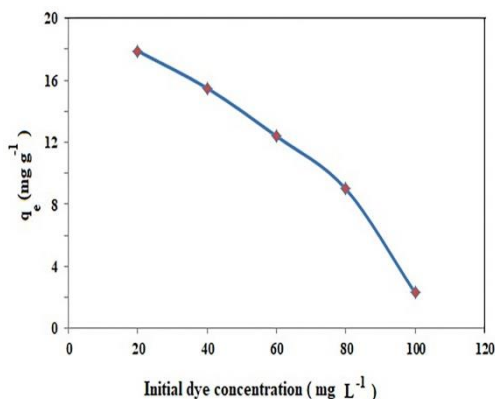


Fig. 9: The effect of initial dye concentration on the adsorption of malachite green through Fe₃O₄/polystyrene-alginate nanocomposite.

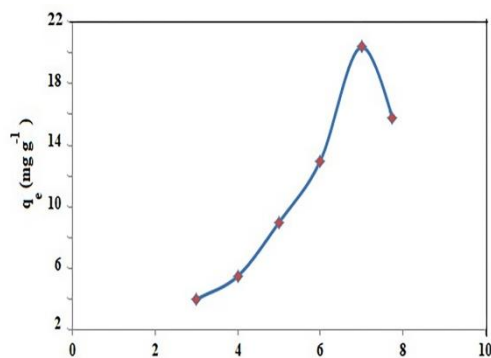


Fig. 10: Varying of adsorbed malachite green with initial pH.

(because of OH⁻ ions) which enhances the electrostatic scattering between the malachite green cations and the adsorbent surface. At acidic pH, the number of H⁺ ions enhances in the media and competes with malachite green as a cationic dye. This can decrease the adsorption of pollutant. In fact, by increasing the pH from 3 to 7, the competition between H⁺ ions and cationic ions of dye declines and cationic dye mainly occupies adsorbent sites. Investigations have proven that at higher pH values, malachite green discoloration enhances because of the reaction of its double bonds with OH⁻ [48]. Therefore, experiments were conducted at optimum pH of 7 to avoid the hydrolysis of dye.

Adsorption isotherm studies

Adsorption isotherms shows the amount of adsorbate that is adsorbed per unit mass of adsorbent as a function of

the equilibrium concentration of the adsorbate at constant temperature (Wang et al., 2018). Various adsorption isotherms, such as Langmuir and Freundlich have been used to explain the equilibrium characteristics of adsorption. In this study, the obtained experimental data were fitted to these adsorption isotherms models in order to verify which model present the best adjustment. The adsorption phenomena occur because of the specific properties of the solid surface that generally comes from two sources [49]:

1) Discontinuity: Absorbent surface nature is significantly different from the bulk properties of adsorbents. Actually, atoms on the surface are different from bulk atoms.

2) Unsaturated: That means the solid surface is in an unsaturated state. Thus, the surface molecules tend to reach saturation.

Each of these adsorption isotherms are based on a set of assumptions.

The Langmuir theory assumes that adsorption occurs at special homogeneous sites on the surface of the adsorbent and suggests the monolayer coverage of the adsorption on the surface of the adsorbent [50].

The Langmuir isotherm model can be represented by the equation (6).

$$\frac{1}{q_e} = \left(\frac{1}{K_L q_m} \right) \frac{1}{C_e} + \frac{1}{q_m} \quad (6)$$

The Freundlich isotherm model assumes that adsorption occurs at heterogeneous surface that is used to describe a multi-layer absorption with interaction between adsorbed molecules [51].

Freundlich theory is describe by the Equation (7):

$$\ln q_e = \frac{1}{n} \ln C_e + \ln K_F \quad (7)$$

Where C_e (mg/L) is the equilibrium concentration of malachite green, q_e (mg/g) is the amount of malachite green adsorbed at equilibrium, q_m (mg/g) is the maximum adsorption at monolayer and K_L (L/mg) is the Langmuir constant including the affinity of binding sites. K_F [(mg/g) (L/mg)^{1/n}] and n are the Freundlich constants showing adsorption capacity and intensity, respectively. To investigate the equilibrium isotherm, in the first stage, UV-Vis spectra obtained during malachite green decolorization with Fe₃O₄/polystyrene-alginate nanocomposite at the various adsorption concentrations. In the

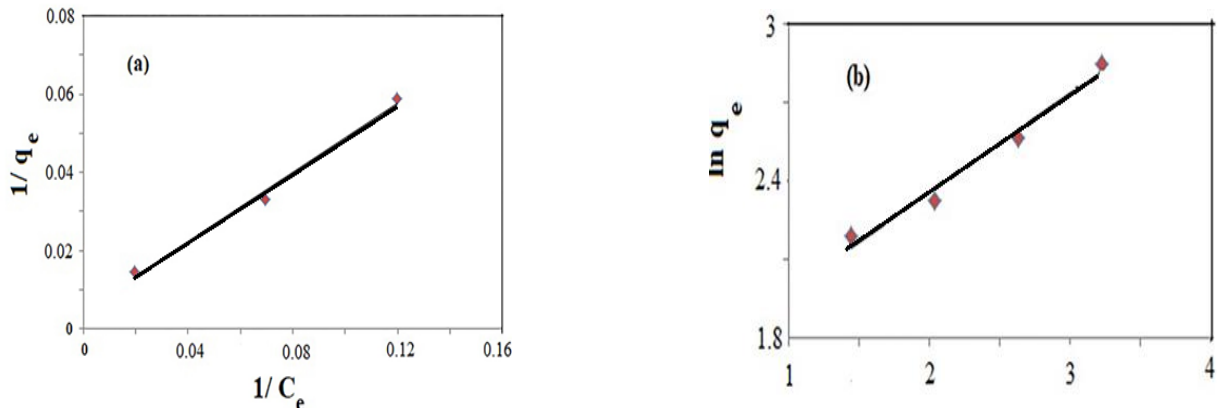


Fig. 9: The effect of initial dye concentration on the adsorption of malachite green through Fe₃O₄/polystyrene-alginate nanocomposite.

Table 3: Isotherm parameters for malachite green adsorption onto Fe₃O₄/polystyrene-alginate nanocomposite.

Type of isotherm model	Value
Langmuir isotherm	
q_m (mg g ⁻¹)	90.81
K_L (L mg ⁻¹)	0.06
R_L	0.29-0.625
R^2	0.996
Freundlich isotherm	
K_F (mg g ⁻¹)	1.32
n	1.59
R^2	0.972

second stage, by calculating concentrations, the values of Langmuir and Freundlich parameters were estimated from the slope and intercept of linear plots of $1/q_e$ versus $1/C_e$ and $\ln q_e$ versus $\ln C_e$ respectively, at 25 °C. Fig. 11 shows the adsorption isotherms plots. From the slopes and intercepts, the values of q_m , K_L , n and K_F were calculated and exhibited in Table 3.

It can be observed from Table 3 that the adsorption procedure could be described via all models from comparing the results of the correlation coefficient values. However, careful observation may explain Langmuir isotherm better than other. As can be observed in Table 1, the obtained correlation coefficient for Langmuir isotherm model was higher than that of other models, which shows the suitability of Langmuir isotherm model for explaining adsorption of malachite green onto Fe₃O₄/polystyrene-

alginate nanocomposite. Based on Langmuir model, the maximum adsorption capacity of Fe₃O₄/polystyrene-alginate nanocomposite for the adsorption of malachite green was found to be 90.81 mg/g. Essential features of Langmuir isotherm model can be defined in term of separation parameter, R_L , as below equation [52]:

$$R_L = \frac{1}{1 + K_L C_0} \quad (8)$$

Where C_0 (mg/L) is the initial pollutant concentration.

The values of R_L arranged as $R_L = 0$, $0 < R_L < 1$ and $R_L > 1$ suggest that adsorption is irreversible, favorable and unfavorable, respectively. Table 3 indicates that R_L values are between 0.29 and 0.625, which implies the adsorption of malachite green onto Fe₃O₄/polystyrene-alginate nanocomposite is favorable.

Thermodynamic study

The thermodynamic investigation was performed by varying the solution temperature between 25 and 40 °C (298–313 K). The free energy change or Gibbs free energy (ΔG^0) (kJ/mol), enthalpy change (ΔH^0) (kJ/mol) and entropy change (ΔS^0) (kJ/mol.K) for the adsorption of malachite green were calculated through Eqs. (9) and (10):

$$\Delta G^0 = -RT \ln K_D \quad (9)$$

$$\ln K_D = \left(\frac{\Delta S^0}{R} \right) - \left(\frac{\Delta H^0}{RT} \right) \quad (10)$$

Where R , T (K) and K_D (q_e/C_e) are the universal gas constant, temperature and the distribution coefficient, respectively [53]. To investigate the thermodynamic

Table 4: The results of thermodynamic study for the adsorption of malachite green onto Fe₃O₄/polystyrene-alginate nanocomposite.

Temperature (K)	(ΔG°) (kJ/mol)	(ΔS°) (kJ/mol.K)	(ΔH°) (kJ/mol)
298	-1.51	-0.034	-11.83
303	-1.36	-	-
308	-1.17	-	-
313	-0.99	-	-

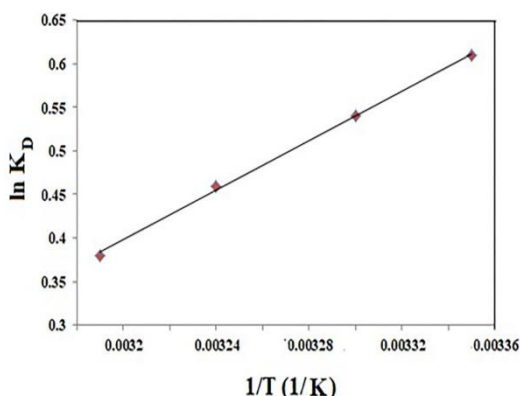


Fig. 12: Thermodynamic profile for malachite green adsorption onto Fe₃O₄/polystyrene-alginate nanocomposite.

of malachite green adsorption onto Fe₃O₄/polystyrene-alginate nanocomposite, thermodynamic constants such as ΔG° , ΔH° and ΔS° were estimated using Eqs. (9) and (10). From the slope ($-\Delta H^\circ/R$) and intercept ($\Delta S^\circ/R$) of the plot of $\ln K_D$ versus $1/T$, the ΔH° and ΔS° of adsorption were calculated, respectively (Fig. 12). The values of these parameters are summarized in Table 4. Table 4 shows the negative ΔG° values, implying the spontaneous nature of the adsorption of malachite green dye [54]. A negative ΔH° shows an exothermic adsorption process for malachite green dye. The negative value of ΔS° indicates the decrease in the degree of freedom of adsorbed malachite green on the binding sites of the nanocomposite at the solid–solution interface, indicating a strong binding of dye ions onto the active sites [55].

CONCLUSIONS

Fe₃O₄/polystyrene-alginate nanocomposite was successfully prepared and was employed as an efficient catalyst for the adsorption of malachite green. The results showed that Fe₃O₄/polystyrene-alginate nanocomposite

is more effective in the comparison with Fe₃O₄, and Fe₃O₄/polystyrene catalysts. Scanning electron microscope analysis proved a homogeneous morphology for prepared nanocomposite which achieved by alginate acting as a stabiliser for Fe₃O₄/polystyrene in the solution state, which in turn avoids the nanoparticles from aggregation. Adsorption is found to depend on contact time, adsorbent dosage, dye Concentration, and pH. The initial pH solution has a marked effect on the malachite green adsorption performance. Kinetic data revealed that the dynamic tendency of malachite green adsorption could be described via pseudo-second-order kinetic model. Equilibrium adsorption data were correlated with Langmuir, and Freundlich adsorption isotherm equations. Isotherm investigations showed that Langmuir model has well explained the equilibrium data of malachite green. The maximum adsorption capacities (q_m) calculated with the Langmuir isotherm model was 90.81 mg/g. Thermodynamic studies demonstrated that the malachite green dye adsorption by Fe₃O₄/polystyrene-alginate nanocomposite was exothermic and spontaneous in nature. Because of the results and advantages expressed, Fe₃O₄/polystyrene-alginate nanocomposite, as one of the good absorbents with high ability has been introduced to remove malachite green dye from aqueous solutions.

Acknowledgments

The authors acknowledge the support of Payame Noor University of Iran.

Received: May. 7, 2022 ; Accepted: Sep. 19, 2022

REFERENCES

- [1] Giahi M., Rahbar A., Mehdizadeh K., [Photochemical Degradation of an Environmental Pollutant by Pure ZnO and MgO Doped ZnO Nanocatalysts](#), *Iran. J. Chem. Chem. Eng.(IJCCE)*, **40(1)**: 83-91 (2021).
- [2] Piramoon S., Aberoomand Azar P., Tehrani M. S., Mohamadi Azar S., [Optimization of Solar-Photocatalytic Degradation of Polychlorinated Biphenyls Using Photocatalyst \(Nd/Pd/TiO₂\) by Taguchi Technique and Detection by Solid Phase Nano Extraction](#), *Iran. J. Chem. Chem. Eng. (IJCCE)*, **40**: 1541-1553 (2021).

- [3] Fekri M.H., Banimahd Keivani M., Razavi Mehr M., Akbari-Adergani B., [Effective Parameters on Removal of Rhodamine B from Colored Wastewater by Nano polyaniline/Sawdust Composite](#), *J. Mazandaran Univ. Med. Sci.*, **29** (177): 166-179 (2019).
- [4] Hamidani M., Djerad S., Tifouti L., [Reactivity of Cu₂O-Cu in the Discoloration of Methylene Blue via a Heterogeneous Fenton-Like Process](#), *Iran. J. Chem. Chem. Eng. (IJCCE)*, **40**: 1502-1511 (2021).
- [5] Fekri M. H., Banimahd keivani M., Darvishpour M., Banimahd keivani H., [Application of Electroactive Nano Composite Coated onto Wood Sawdust for the Removal of Malachite Green Dye from Textile Wastewaters](#), *J. Phys. Theor. Chem.*, **9**(2): 95-102 (2012).
- [6] Shirzad Taghanaki N., Keramati N., Mehdipour M., [Photocatalytic Degradation of Ethylbenzene by Nano Photocatalyst in Aerogel form Based on Titania](#), *Iran. J. Chem. Chem. Eng. (IJCCE)*, **40**(2): 525-537 (2021).
- [7] Di Mauroa A., Cantarella M., Nicotra G., Privitera V., Impellizzeri G., Impellizzeri, G. [Low Temperature Atomic Layer Deposition of ZnO: Applications in Photocatalysis](#), *Appl. Catal. B-Environ.*, **196**: 68–76 (2016).
- [8] Ding M., Chen W., Xu H., Shen Z., Lin T.; Hu, K., Kong Q., Yang G., Xie Z., [Heterogeneous Fe₂CoTi₃O₁₀- MXene Composite Catalysts: Synergistic Effect of the Ternary Transition Metals in the Degradation of 2,4- Dichlorophenoxyacetic Acid Based on Peroxymonosulfate Activation](#), *Chem. Eng. J.*, **378**: 122177–122187 (2019).
- [9] Li J., Zhang L., [3D Pothole-Rich Hierarchical Carbon Framework-Encapsulated Ni Nanoparticles for Highly Selective Nonenzymatic Cysteine Detection](#), *Electrochim. Acta.*, **328**: 135126–135134 (2019).
- [10] Goswami B., Mahanta D., [Fe₃O₄-Polyaniline Nanocomposite for Non-enzymatic Electrochemical Detection of 2,4-Dichlorophenoxyacetic Acid](#), *ACS Omega.*, **6**: 17239–17246 (2021).
- [11] Azimi S., Shirini F., Pendashteh A., [Advanced Oxidation Process as a Green Technology for Dyes Removal from Wastewater: A Review](#), *Iran. J. Chem. Chem. Eng. (IJCCE)*, **40**: 1467-1489 (2021).
- [12] Mohammadi R., Massoumi B., Emamalinasabb B., Eskandarloo H., [Cu-doped TiO₂-graphene/alginate Nanocomposite for Adsorption and Photocatalytic Degradation of Methylene Blue from Aqueous Solutions](#), *Desal. Wat. Treat.*, **82**: 81–91 (2017).
- [13] Pervez N., He W., Zarra T., Naddeo V., Zhao Y., [New Sustainable Approach for the Production of Fe₃O₄/Graphene Oxide-Activated Persulfate System for Dye Removal in Real Wastewater](#), *Water.*, **12**: 733-749 (2020).
- [14] Hammouda S. B., Adhoum N., Monser L., [Synthesis of Magnetic Alginate Beads Based on Fe₃O₄ Nanoparticles for the Removal of 3-Methylindole from Aqueous Solution Using Fenton Process](#), *J. Hazard. Mater.*, **294**: 128–136 (2015).
- [15] Toktam P., Es'haghi Z., Ahmadpour A., Nakhaei A., [Optimization of Adsorption Parameters Using Central Composite Design for the Removal of Organosulfur in Diesel Fuel by Bentonite-Supported Nanoscale NiO-WO₃](#), *Iran.J. Chem. Chem. Eng. (IJCCE)*, **41**: 808-820 (2022).
- [16] Kong M., Chen X.G., Xing K., Park H.J., [Antimicrobial Properties of Chitosan and Mode of Action: A State of the Art Review](#), *Int. J. Food Microbiol.*, **144**: 51–63 (2010).
- [17] Pervez M.N., He W., Zarra T., Naddeo V., Zhao Y., [New Sustainable Approach for the Production of Fe₃O₄/Graphene Oxide-Activated Persulfate System for Dye Removal in Real Wastewater](#), *Water.*, **12**: 733-750 (2020).
- [18] Yu D., Wu M., Hu Q., Wang L., Lv C., Zhang L., [Iron-Based Metal-Organic Frameworks as Novel Platforms for Catalytic Ozonation of Organic Pollutant: Efficiency and Mechanism](#), *J. Hazard. Mater.*, **367**: 456–464 (2019).
- [19] Liu Z., Li X., Rao Z., Hu F., [Treatment of Landfill Leachate Biochemical Effluent Using the Nano-Fe₃O₄ /Na₂S₂O₈ System: Oxidation Performance, Wastewater Spectral Analysis, and Activator Characterization](#), *J. Environ. Manag.*, **208**: 159–168 (2018).
- [20] Ghasemi S.S., Hadavifar M., Maleki B., Mohammadnia E., [Adsorption of Mercury Ions from Synthetic Aqueous Solution Using Polydopamine Decorated SWCNTs](#), *J. Water Process. Eng.*, **32**: 100965 (2019).
- [21] Mohammadi L., Rahdar A., Khaksefidi R., Ghamkhari A., Fytianos G., Kyzas G.Z., [Polystyrene Magnetic Nanocomposites as Antibiotic Adsorbents](#), *Polymers.*, **12**: 1313-1321 (2020).
- [22] Ren L., Yang Z., Huang L., He Y., Wang H., Zhang L., [Macroscopic Poly Schiff Base-Coated Bacteria Cellulose With High Adsorption Performance](#), *Polymers.*, **12**: 714-728 (2020).

- [23] Laurent S., Forge D., Port M., Roch A., Robic C., Elst L., Muller R., [Magnetic Iron Oxide Nanoparticles: Synthesis, Stabilization, Vectorization](#), *J. Hazard. Mater.*, **294**: 128–136 (2015).
- [24] Habibi-Yangjeh A., Shekofteh-Gohari M., [Synthesis of Magnetically Recoverable Visible-Light-Induced Photocatalysts by Combination of Fe₃O₄/ZnO with BiOI and Polyaniline](#), *Pro. Nat. Sci. Mater. Int.*, **29**: 145–155 (2019).
- [25] Liu M., Liu Y., Ge Y., Zhong Z., Wang Z., Wu T., Zhao X., Zu Y., [Solubility, Antioxidation, and Oral Bioavailability Improvement of Mangiferin Microparticles Prepared Using the Supercritical Antisolvent Method](#), *Pharmaceutics*, **12**: 90-105 (2020).
- [26] Belattmania Z., Kaidi S., El Atouani S., Katif C., Bentiss F., Jama C., Reani A., Sabour B., Vasconcelos V., [Isolation and FTIR-ATR and ¹H NMR Characterization of Alginates from the Main Alginophyte Species of the Atlantic Coast of Morocco](#), *Molecules*, **25**: 4335-4343 (2020).
- [27] Fekri M. H., Tousi F., Heydari R., Razavi Mehr M., Rashidipour M., [Synthesis of Magnetic Novel Hybrid Nanocomposite \(Fe₃O₄@SiO₂/Activated Carbon\) by a Green Method and Evaluation of Its Antibacterial Potential](#), *Iran. J. Chem. Chem. Eng. (IJCCE)*, **41**: 767-776 (2022).
- [28] Salamat S., Mohammadnia E., Hadavifar M., [Kinetics and Adsorption Investigation of Malachite Green onto Thiolated Graphene Oxide Nanostructures](#), *J. Wat. Wastewat.*, **31**: 1-11 (2020).
- [29] Niu H., Dizhang Z., Meng Y., Cai H., [Fast Defluorination and Removal of Norfloxacin by Alginate/Fe@Fe₃O₄ Core/shell Structured Nanoparticles](#), *J. Hazard. Mater.*, **227**: 195–203 (2020).
- [30] Honga R.Y., Fenga B., Liua G., Wangc S., Li H.Z., Ding J.M., Zhenge Y., Weif D.G., [Preparation and Characterization of Fe₃O₄/polystyrene Composite Particles Via Inverse Emulsion Polymerization](#), *J. Alloys Compd.*, **476**: 612–618 (2009).
- [31] Rajendrachari S., Cahit Karaoglanli A., Ceylan Y., Uzun O., [A Fast and Robust Approach for the Green Synthesis of Spherical Magnetite \(Fe₃O₄\) Nanoparticles by Tilia tomentosa \(Ihlamur\) Leaves and its Antibacterial Studies](#), *Pharm. Sci.*, **26(2)**: 175-183 (2020).
- [32] Shah R M. T., Balouchb A., Alveroglu E., [Sensitive Fluorescence Detection of Ni²⁺ Ions Using Fluorescein Functionalized Fe₃O₄ Nanoparticles](#), *J. Mater. Chem. C.*, **6**: 1105-1115 (2018).
- [33] Wan S., Huang J., Yan H., Liu K., [Size-Controlled Preparation of Magnetite Nanoparticles in the Presence of Graft Copolymers](#), *J. Mater. Chem.*, **16**: 298–303 (2006).
- [34] Ghamkhari A., Mohamadi L., Kazemzadeh S., Zafar M.N., Rahdar A., Khaksefidi R. [Synthesis and Characterization of poly\(Styrene-Block-Acrylic acid\) Diblock Copolymer Modified Magnetite Nanocomposite for Efficient Removal of Penicillin G](#), *Compos. Part B-Eng.*, **182**: 107643 (2020).
- [35] Liang H., Hu X., [Preparation of Magnetic Cellulose Nanocrystal -Modified Diatomite for Removal of Methylene Blue from Aqueous Solutions](#), *Iran. J. Chem. Chem. Eng. (IJCCE)*, **41**: 787-798 (2022).
- [36] Ohsawa K, Murata M., Ohshima H., [Zeta Potential and Surface Charge Density of Polystyrene-Latex; Comparison with Synaptic Vesicle and Brush Border Membrane Vesicle](#), *Colloid Polym. Sci.*, **264**: 1005–1009 (1986).
- [37] Parlayici Ş., [Alginate-Coated Perlite Beads for the Efficient Removal of Methylene Blue, Malachite Green, And Methyl Violet from Aqueous Solutions: Kinetic, Thermodynamic, and Equilibrium Studies](#), *Parlayici. J. Anal. Sci. Technol.*, **10**: 4 (2019).
- [38] Yang L., Tian J., Meng J., Zhao R., Li C., Ma J., Jin T., [Modification and Characterization of Fe₃O₄ Nanoparticles for Use in Adsorption of Alkaloids](#), *Molecules*, **23**: 562-571 (2018).
- [39] Bao S.G., Tang L.H., Li K., Ning P., Peng J.H., Guo H.B., Zhu T.T., Liu Y., [Highly Selective Removal of Zn\(II\) Ion From Hot-Dip Galvanizing Pickling Waste with Amino-Functionalized Fe₃O₄@SiO₂ Magnetic Nano-Adsorbent](#), *J. Colloid Interface Sci.*, **462**: 235–242 (2016).
- [40] Bao S.G., Li K., Ning P., Peng J.H., Jin X., Tang L.H., [Highly Selective Removal of Mercury and Lead Ions from Wastewater by Mercaptoamine-Functionalised Silica-Coated Magnetic Nano-Adsorbents: Behaviours and Mechanisms](#), *Appl. Surf. Sci.*, **393**: 457–466 (2017).

- [41] Rahmani A., Zavvar Mousavi H., Fazli M., [Effect of Nanostructure Alumina on Adsorption of Heavy Metals](#), *Desalination*, **253**: 94–100 (2010).
- [42] Xu R., Mao J., Peng N., Luo X., Chang C., [Chitin/clay Microspheres with Hierarchical Architecture for Highly Efficient Removal of Organic Dyes](#), *Carbohydr. Polym.*, **188**: 143–150 (2018).
- [43] Shi X., Zhang X., Ma L., Xiang C., Li L.L., [TiO₂-Doped Chitosan Microspheres Supported on Cellulose Acetate Fibers for Adsorption and Photocatalytic Degradation of Methyl Orange](#), *Polymers.*, **11**:1293 (2019).
- [44] Rahimi K., Mirzaei R., Akbari A., Mirghaffari N., [Preparation of Nanoparticle-Modified Polymeric Adsorbent Using Wastage Fuzzes of Mechanized Carpet And its Application in Dye Removal from Aqueous Solution](#), *J. Clean. Prod.*, **178**: 373–383 (2017).
- [45] Wang P.P., Wang L.H., Dong S.J., Zhang G.H., Shi X.J., Xiang C.H., Li, L.L., [Adsorption of Hexavalent Chromium By Chitosan/poly\(ethylene oxide\)/permutit Electrospun Fibers](#), *New. J. Chem.*, **42**: 17740–17749 (2018).
- [46] Mane V. S., Mall I. D., Srivastava V. C., [Kinetic and Equilibrium Isotherm Studies for the Adsorptive Removal of Brilliant Green Dye from Aqueous Solution by Rice Husk ash](#), *J. Environ. Manage.*, **84**: 390-400 (2007).
- [47] Mohammadi R., Massoumi B., Galandar F., [Polyaniline-TiO₂/Graphene Nanocomposite: An Efficient Catalyst for the Removal of Anionic Dyes](#), *Desal. Wat. Treat.*, **142**: 321–330 (2019).
- [48] Lam S.W., Soetanto A., Amal R., [Self-Cleaning Performance of Polycarbonate Surfaces Coated with Titania Nanoparticles](#), *J. Nanoparticle Res.*, **11**: 1971–1979 (2009).
- [49] Ngomsik A. F., Bee A., Talbot D., Cote G., [Magnetic Solid-Liquid Extraction of Eu \(III\), La \(III\), Ni \(II\) and Co\(II\) with Maghemite Nanoparticles](#), *Sep. Purif. Technol.*, **86**: 1-8 (2012).
- [50] Ribeiro R.S., Fathy N.A., Attia A.A., Silva A.M.T., Faria J.L., Gomes H.T., [Activated Carbon Xerogels for the Removal of the Anionic Azo Dyes Orange II and Chromotrope 2R by Adsorption and Catalytic Wet Peroxide Oxidation](#), *Chem. Eng. J.*, **195**: 112-121 (2012).
- [51] Pervez M. N., He W., Zarra T., Naddeo V., Zhao Y., [New Sustainable Approach for the Production of Fe₃O₄/Graphene Oxide-Activated Persulfate System for Dye Removal in Real Wastewater](#), *Water.*, **12**: 733-750 (2020).
- [52] Ahmadi S., Igwegbe C.A., Rahdar S., [The application of Thermally Activated Persulfate for Degradation of Acid Blue 92 in Aqueous Solution](#), *Int. J. Ind. Chem.*, **10**: 1–12 (2019).
- [53] Bendjama H., Merouani S., Hamdaoui O., Bouhelassa M., [Using Photoactivated Acetone for the Degradation of Chlorazol Black in Aqueous Solutions: Impact of Mineral and Organic Additives](#), *Sci. Total. Environ.*, **653**: 833–838 (2019).
- [54] Singh S., Singh P.K., Mahalingam H., [Novel floating Ag⁺ - Doped TiO₂ /Polystyrene Photocatalysts for the Treatment of Dye Wastewater](#), *Ind. Eng. Chem. Res.*, **53**: 16332–16340 (2014).
- [55] Idris A., Ismail N.S.M., Hassan N., Misran E., Ngomsik A.F., [Synthesis of Magnetic Alginate Beads Based on Maghemite Nanoparticles for Pb \(II\) Removal in Aqueous Solution](#), *J. Ind. Eng. Chem.*, **18**: 1582–1589 (2012).